Journal of Applied Electrochemistry **33**: 355–360, 2003.

Preparation and characterization of polyaniline powder synthesized on microstructured aluminium

D. HUERTA-VILCA, S.R. MORAES and A.J. MOTHEO*
Departamento de Físico-Química, Instituto de Química de São Carlos, Universidade de São Paulo, CP 780, São Carlos, SP 13560-970, Brazil
*(*author for correspondence, e-mail: artur@iqsc.sc.usp.br)*

Received 24 July 2002; accepted in revised form 2 January 2003

Key words: aluminium, conducting polymer, polyaniline, powder

Abstract

Aluminium surfaces were microstructured in 0.1 M HNO_3 by potentiodynamic anodic activation to potentials generating pitting. This surface was then used as an electrode to prepare polyaniline powder. The number of pits is responsible for the amount of powder produced. Emeraldine salt powder was successfully prepared from 0.4 M aniline in 0.5 M H_2SO_4 solution. Other acid solutions for deposition are not convenient because powders are electrochemically inactive (e.g., in 1 M HNO_3) or the electrode is covered by a film (e.g., in 0.5 M $H_2C_2O_4$).

1. Introduction

Conducting polymers have been tested as cathodic materials in lithium secondary batteries, and they are generally synthesized chemically [1–6]. Chemical synthesis of polyaniline (PAni) using oxidants causes recycling problems, as well as contamination of the product. However, battery quality polymer powders can be prepared by electrodeposition [7].

Since 1988, polymers have been deposited on active metals such as iron and aluminium [8]. Specifically in that study, potentiodynamic anodic activation of aluminium was performed in 0.1 M HNO_3, in the absence and presence of 0.1 M pyrrole, with a scan rate of 2 mV s^{-1}. By using this superficial pretreatment, a pitted electrode filled with electrolyte or polypyrrole was obtained. This electrode was successively used to prepare battery-grade polypyrrole powder. In another study, the same authors performed a galvanostatic anodic activation of aluminium in 0.1 M HNO_3 with 0.1 M pyrrole at 25 mA cm^{-2} for 2 min, before electrodeposition of polypyrrole was performed. Galvanostatic deposition of polypyrrole at 0.5 mA cm^{-2} for 38 min from 0.8 M pyrrole in a chelating acid such as 0.1 M $H_2C_2O_4$ produced a strongly adherent film [9]. Both studies showed that anodic, potentiodynamic or galvanostatic activation of aluminium at a potential above the pitting potential produces a microstructured aluminium surface. This microstructured surface has the capability to be used for either polymer powder production in a strong acid solution or polymer film formation in a chelating acid solution.

Nanostructuring of aluminium to prepare porous alumina membranes and its use in the deposition of different materials (metals, semiconductors, polymers, catalysts) is well known in template-synthesis [10, 11]. This technique has become important to prepare PAni nanofibrils. Recently, iron nanowires encapsulated in PAni nanotubules have been prepared inside the pores of the alumina template [12].

The aim of the present work is to describe an electrochemical method to prepare PAni-powder from aqueous acid solution, on a substrate consisting of microstructured aluminium. Aluminium was preferred as the substrate because in the potential range of PAni deposition, most of the active metals dissolve anodically to form passive films and the microstructure would be damaged during polymerisation.

2. Experimental details

Aluminium discs of 1 cm^2 were used as electrodes. A Pt wire was spot-welded on the backside of the Al discs to provide an electrical connection and then the samples were embedded in acrylic resin. After polishing with emery paper (320–1200 grade), degreasing in ethanol and drying at 40 °C, the specimens were submitted to anodic activation in 0.1 M HNO_3 containing 0.1 M aniline. The activation was performed potentiodynamically at potentials between 0.2 and 2.0 V at 2 mV s^{-1}. After anodic activation, the specimens were characterized by electrochemical impedance spectroscopy. A single compartment electrochemical cell, with a platinum foil (2 cm × 2 cm) as counter electrode and a saturated calomel electrode (SCE) as reference, was used.

Aniline was predistilled over zinc dust to remove the oxidation impurities. The deposition electrolytes were: 0.4 M aniline in 0.5 M H_2SO_4 or 0.8 M aniline in 1 M HNO_3. The electropolymerisation of PAni is performed in a potential window between −0.2 and +0.8 V vs SCE. To obtain non-overoxidized PAni powder, which normally occurs at potentials higher than 1.0 V vs SCE, the potential was monitored during the electrodepositions. All electrolytes were prepared by using Milli-Q water.

The measuring equipment was a potentiostat/galvanostat (273A, EG&G) connected to a frequency response analyser (FRA 1255, Solartron) for the impedance measurements. The activated surface was characterized by electrochemical impedance spectroscopy (EIS) and the surface topography by scanning electron microscopy (SEM).

The accumulated powder at the bottom of the cell was separated by filtration and washed with 1 M HCl solution. After filtration, the powder was dried under a dynamic vacuum. This was followed by de-doping in 0.1 M NH_4OH solution for 20 h under agitation to neutralise the acid in the polymer. After de-doping, the powder was filtered and dried again under a dynamic vacuum, and finally stored under vacuum until analysis. PAni samples were characterized by u.v.–visible spectroscopy. First spectra of de-doped PAni were recorder in 5% solutions of de-doped PAni (emeraldine base) solution in *N*-methyl-pyrrolidinone (NMP). Thereafter, droplets of 1 M HCl solution were added to the emeraldine base solution, and the doped PAni spectra were measured. For the analysis by infrared spectroscopy, each sample powder was mixed with KBr by thorough grinding and pressed into a transparent disc.

3. Results and discussion

It is well known that pitting of aluminium in nitric acid solution at 1.78 V vs SCE, which is indicated by a steep current rise [13]. Figure 1 shows the potentiodynamic activation curves for aluminium above the pitting potential in 0.1 M HNO_3 with and without aniline. An initial current decay due to passivation can be observed, whose current densities are around 0.1 mA cm^{-2} for 0.1 M HNO_3 with 0.1 M aniline and around 1 mA cm^{-2} for the monomer-free acid solution, are maintained until pitting potentials are reached. It is obvious that the aniline in the solution enhances the passivation. By examining the surface after the first potentiodynamic activation sweep in 0.1 M HNO_3 with 0.1 M aniline, a small number of pits was observed on the anodised surface. Four more activation sweeps produced a large number of pits filled with PAni.

The idea of using a prepared surface with sufficient number of pits as a precipitation electrode is based on the fact that the polymerization process takes place preferentially on PAni-filled pits, and film formation is avoided. From each precipitation site, the polymer falls under the action of gravity to the bottom of the cell.

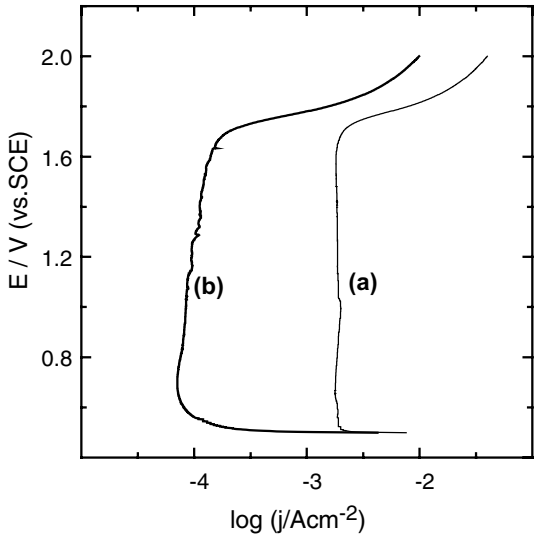

Fig. 1. Potentiodynamic anodic activation of aluminium in 0.1 M HNO_3 (a) without and (b) with 0.1 M aniline. Scan rate 2 mV s^{-1}.

Cary et al. [14] used the same idea to prepare microporous alumina films at electrodes. The structure of the oxide film produced in this way consists of an array of parallel cylindrical pores normal to the oxide surface. The authors observed that the thickness of the porous aluminium oxide increased linearly with anodisation time at a given voltage and temperature and the diameter if the porous can be adjusted from 0.1 to 10 μm.

PAni powder obtained galvanostatically at 1–4 mA cm^{-2} from both 0.4 M aniline in 0.5 H_2SO_4 and 0.8 M aniline in 1 M HNO_3 presented similar morphology. Although the solution of 1 M HNO_3 with 0.8 M aniline turns red with increasing number of galvanostatic depositions, the composition of the electrolyte, 0.5 M H_2SO_4 with 0.4 M aniline remains unchanged. The colour changes of the HNO_3 solutions are attributed to the formation of soluble aniline oligomers in the electrolyte.

The efficiency of the polymerization can be estimated by the method established by Schirmeisen and Beck [15]. The current efficiency, γ, is defined as the ratio of the experimental, $m_{e,exp}$, and theoretical, $m_{e,th}$, electrochemical equivalent as

$$\gamma = \frac{m_{e,\exp}}{m_{e,th}}$$

where $m_{e,th}$ for PAni was calculated, considering high degree of polymerization, as

$$m_{e,th} = \frac{M}{zF} = \frac{M_M + yM_A}{(2+y)F}$$

where M_M is the molecular weight of the monomer in the polymer ($M_M = M_{An} - 2 = 91$), M_A is the molecular weight of the anion (for the sulfate ion $M_A = 96$), y is a stoichiometric factor (degree of insertion) and F

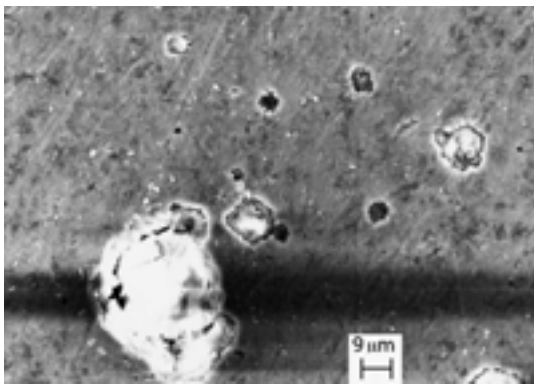

Fig. 2. SEM micrograph of aluminium surface anodically activated in 0.1 M HNO_3 with 0.1 M aniline after usage for powder deposition.

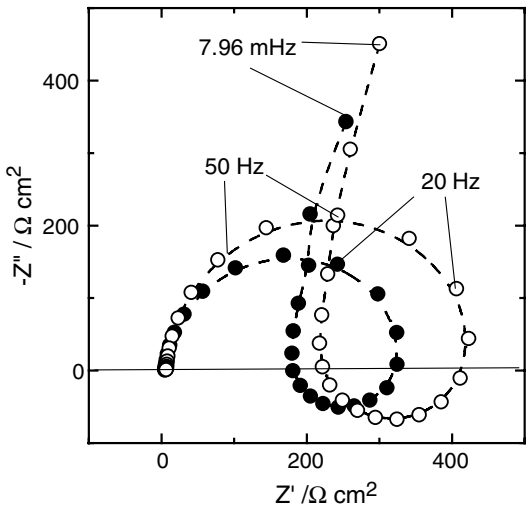

Fig. 3. Nyquist plots of microstructured aluminium surface by anodic activation in 0.1 M HNO_3 (○) without and (●) with addition of 0.1 M aniline. Impedance spectra taken in 0.5 M $H_2C_2O_4$ solution at $E = 0.6$ V vs SCE.

is the faradaic constant (96 490 C mol^{-1}). So, assuming $y = 0.25$, the value of $m_{e,th}$ can be evaluated as 0.530 mg C^{-1}.

The resulting mass of PAni powder obtained in sulfuric acid solution after the application of five successive galvanostatic (1 mA) depositions of 500 s each was 0.5 mg, which corresponds to an electrochemical equivalent equal to 0.2 mg C^{-1}. So the current efficiency for the PAni deposition from sulfuric acid solution is 37.7%. In the same way, a current efficiency of 62.2% is obtained for deposition from nitric acid solution.

In Figure 2, the SEM-micrograph of the aluminium surface anodically preactivated in 0.1 M HNO_3 containing 0.1 M aniline solution clearly shows pits filled with PAni. Inside empty pits, parasite faradaic processes can occur, causing the accumulation of corrosion products. An example is the largest pit with white scale in Figure 2. PAni-filled pits of similar diameter should be observed in the case of an optimum microstructured surface.

To analyse better the microstructured aluminium surface, measurements using electrochemical impedance spectroscopy (EIS) were performed with the potentiodynamically microstructured electrodes. The electrochemical impedance spectra of the activated surfaces in monomer-free and monomer-containing 0.1 M HNO_3 solutions showed slight differences in shape. To avoid alteration of the microstructure by corrosion, EIS measurements were performed in 0.5 M $H_2C_2O_4$ solution at $E = 0.6$ V vs SCE, which is close to the open circuit potential. The Nyquist plots in Figure 3 are characterized in both cases by a capacitive semicircle for the charge transfer reaction and a positive inductive loop corresponding to the pits. It can be stated that the charge transfer resistance of the fresh-pitted aluminium surface is around 90 Ω larger than that of the surface containing PAni in the pits. The freshly pitted surface is also less polarizable than the surface with polymer filled pits, because the charge transfer reaction may occur faster through the conductive polymeric material than through the open pits. In addition, the capacity of aluminium with PAni-filled pits (21.63 μF cm^{-2}) is higher than that of aluminium with empty pits (9.87 μF cm^{-2}).

In Figure 4, the surface layermodel, the equivalent circuit and the curve fitting for the potentiodynamically anodized aluminium electrode in 0.1 M HNO_3 containing 0.1 M aniline solution are represented. From the preparation method, a sandwich structure with local nonhomogeneities can be considered to represent the surface, because the multilayer model, as represented in Figure 4(a), is generally accepted for anodized aluminium [16].

For this type of structure, a local nonhomogeneity with a 'passive pit', where the damage is restricted to the outer layer, can be assumed [17]. The transfer function consists of a parallel combination of the undamaged Al-film areas and that of the pore resistance of the outer layer (L_2 in Figure 4(a)), formed by porous oxide, in series to the passive inner layer (L_1 in Figure 4(b)), which consists of barrier oxide. The pseudo-inductance coupled to the pore resistance corresponds to the positive loop in the Nyquist diagram. In Figure 4(c), the optimum data fits along with the experimental results are represented. The fitting parameters are summarised in Table 1.

The oxide parameters, a series of two parallel combinations of constant phase elements (CPE) and resistances, correspond to the data fitting of the undamaged surface. The data points, including the positive semicircle, are fitted with the pore resistance and the combination of pseudo inductance-resistances. To fit the data points at lower frequencies, it was necessary to include a parallel combination of R6 and C1 (CPE was omitted here because the dispersion coefficient was equal to 1), as additional connection, in series.

Comparing the amounts of powder obtained it can be concluded that the powder production in nitric acid solutions has higher current efficiency than in sulphuric

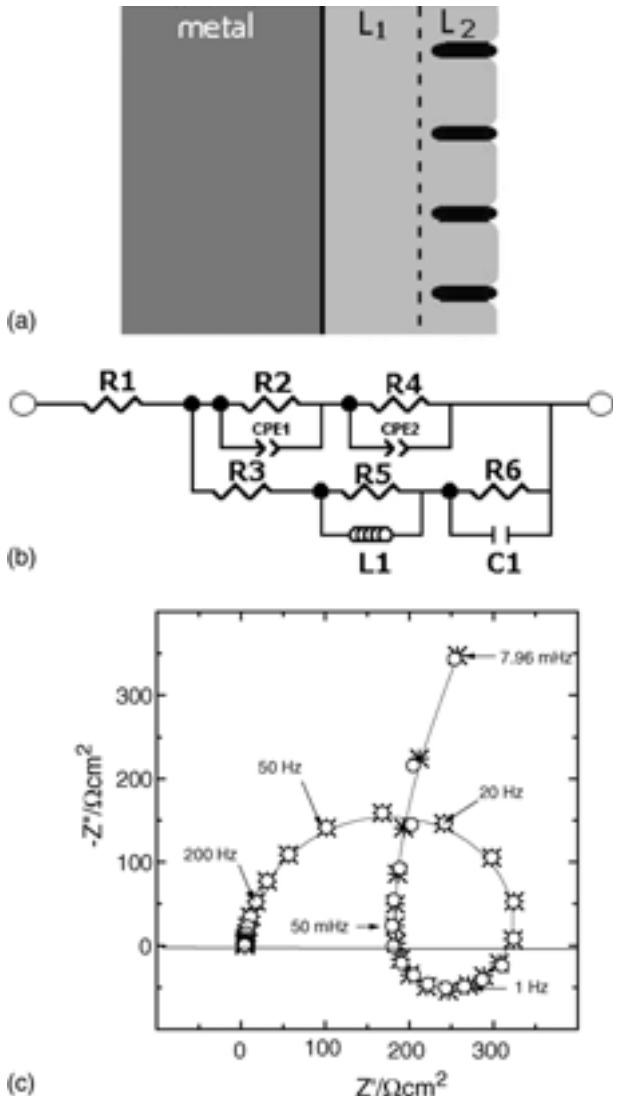

Fig. 4. 3D sandwich layer system representing the electrode side of the interface, containing (a) 'passive pit' model with local damages in the outer layer, (b) equivalent circuit and (c) the impedance spectrum ((◯) experimental results and (∗) fitted points) of aluminium surface obtained after anodic activation in 0.1 M HNO_3 solution with addition of 0.1 M aniline. Impedance spectra taken in 0.5 M $H_2C_2O_4$ solution at $E = 0.6$ V vs SCE.

acid. Falling fine powder within the red turning electrolyte was observed but the powder was nonelectroactive as corroborated by its u.v.–vis. spectrum. By contrast, in sulfuric acid, a green powder was formed and identified as electroactive emeraldine.

The u.v.–vis. spectra of PAni powder produced in H_2SO_4 (Figure 5(a)) indicates that the powder in the undoped state is composed of emeraldine base. Absorption bands at around 325 nm and 620 nm, corresponding to the π–π^* electron transition in the benzene ring and charge transfer from quinoid to benzoid rings, respectively, are observed. After doping with 1 M HCl, bands at 365 nm and 820 nm appear, corresponding to the presence of polarons and bipolarons, respectively. These bands are related to an increase in the conductivity by doping [18]. On the other hand, the precipitated

Table 1. Fitting parameters of anodic preactivated aluminum using the 'passive pit' model describe in Figure 4

	R_1 /Ω	R_2 /Ω	CPE1		R_4 /Ω	CPE2		R_3 /Ω	R_5 /Ω	L_1 /H	R_6 /Ω	C_1 /F
			Y_0 /Ω^{-1}	n_f		Y_0 /Ω^{-1}	n_f					
Al/0.1 M HNO_3	6.57	3075	15.81×10^{-6}	0.94	12614	0.48×10^{-6}	1	218	165	32	3307	35.4×10^{-3}
Al/0.1 M HNO_3 + 0.1 M aniline	4.66	8043	21.76×10^{-6}	0.94	9636	0.76×10^{-6}	1	178	121	27	1886	53.6×10^{-3}

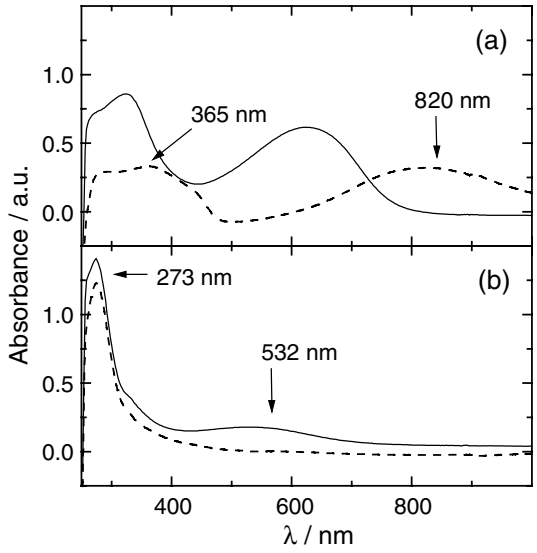

Fig. 5. U.v.–vis. spectra of PAni powder produced in (a) 0.5 M H_2SO_4 + 0.4 M aniline, (b) 1 M HNO_3 + 0.8 M aniline. PAni in undoped state (solid lines) and doped state (dashed line) with 1 M HCl solution.

powder in HNO_3 (Figure 5(b)) is composed of nonelectroactive PAni (pernigraniline). The undoped powder shows absorption bands at 330 nm and 530 nm, which is in agreement with the pernigraniline base bands reported in the literature [19]. The dashed line in Figure 5(b), shows that the doping process in pernigranile base was impossible with 1 M HCl.

The 1 M HNO_3 containing aniline solutions that turned red during the process of powder deposition were evaporated to leave only a reddish powder. This powder was dissolved in NMP and its electronic states were analysed. The u.v.–vis. spectra in Figure 6 demonstrate that the powder is mainly composed by leucoemeraldine

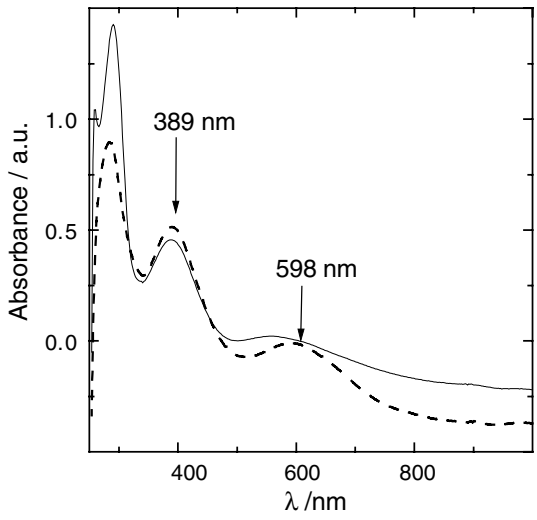

Fig. 6. U.v–vis. spectra of PAni powder produced in 1 M HNO_3 + 0.8 M aniline after evaporation of solution. PAni in undoped state (solid lines) and doped state (dashed line) with 1 M HCl solution.

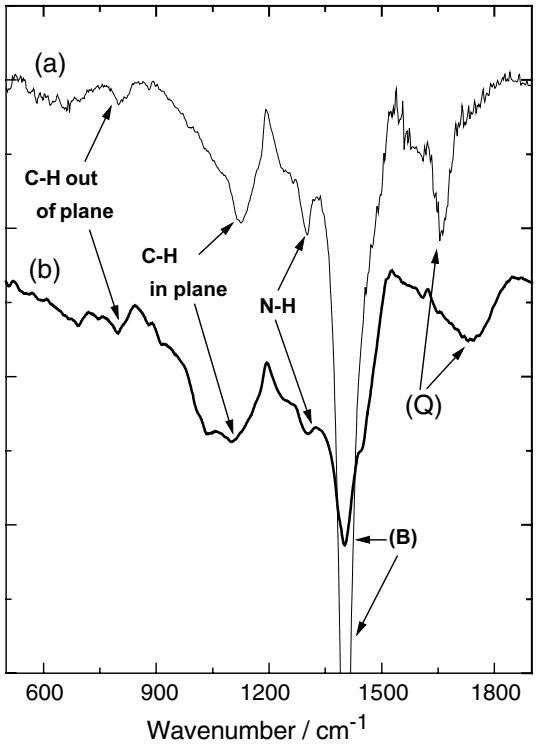

Fig. 7. FTIR spectra of PAni powder obtained from solutions containing aniline and (a) 0.5 M H_2SO_4; (b) 1 M HNO_3.

base (solid line). The doping of the leucoemeraldine base was performed by the addition of 1 M HCl solution and the u.v.–vis. spectrum obtained (Figure 6, dashed line) is compatible with the emeraldine base, reduced form of the leucoemeraldine. This observation is based on the appearance of the band at 290 nm which corresponds to the polaron formation in the emeraldine chain.

In Figure 7, the structural properties of powders formed in 0.5 M H_2SO_4 and 1 M HNO_3 solutions can be compared by the FTIR spectra. Typical bands at around 1600 and 1400 cm^{-1} correspond to stretching vibrations of bonds in quinone and benzoid rings, respectively. Band-shift of quinone (Q) for PAni powder formed in 1 M HNO_3 solution is due to the less energetic doping bonds of NO_3^- anions in the polymer. Bands at around 1300 cm^{-1} correspond to N–H bonds. The bands at around 1100 and 800 cm^{-1} are attributable to C–H vibrations of the ring in plane and out of plane, respectively [20, 21]. From the benzoid/quinoid ratio, it can be stated that both powders were converted to the emeraldine salt form by water absorption. The extremely high benzenoide-peak of the powder prepared in H_2SO_4 probably arises from the highly structured and pure polymer material.

4. Conclusions

An electrochemical route to prepare PAni powder avoiding contamination with oxidants has been demonstrated. The microstructured aluminium surface can be

used in the preparation of PAni powder because the growth, as a uniform polymer layer, is hindered. The number of pits determines the efficiency of the process. Pits are growth centres for PAni, which falls under the action of gravity. PAni powder produced in 0.5 M H_2SO_4 is the most promising and the product consists mainly of emeraldine salt, probably with a high molecular weight.

In principle, such microstructured aluminium offers the possibility of long-term production of powder; however, at this stage, the formation of alumina must be minimized.

Acknowledgement

The financial support of Fundação de Amparo à Pesquisa do Estado de São Paulo (FAPESP Processes 1999/11621-7 and 2000/02674-9) is gratefully acknowledged.

References

1. J.S. Miller, *Adv. Mater.* **5** (1993) 671.
2. J.C. Chiang and A.G. Macdiarmid, *Synth. Met.* **13** (1986) 193.
3. T. Osaka, T. Momma, H. Ito and B. Scrosati, *J. Power Sources* **68** (1997) 392.
4. W.H. Qiu, R.Q. Zhou, L.L. Yang and Q.G. Liu, *Sol. State Ion.* **86-8** (1996) 903.
5. A.J. Motheo, E.C. Venancio and L.H.C. Mattoso, *Electrochim. Acta* **43** (1998) 755.
6. E. Spila, S. Panero and B. Scrosati, *Electrochim. Acta* **43** (1998) 1651.
7. E.C. Venancio, A.J. Motheo, F.A. Amaral and N. Bocchi, *J. Power Sources* **94** (2001) 36.
8. P. Hulser and F. Beck, *J. Electrochem. Soc.* **137** (1990) 2067.
9. P. Hulser and F. Beck, *J. Appl. Electrochem.* **20** (1990) 596.
10. Z.H. Yuan, H. Huang, L. Liu and S.S. Fan, *Chem. Phys. Lett.* **345** (2001) 39.
11. G.L. Hornyak, A.C. Dillon, P.A. Parilla, J.J. Schneider, N. Czap, K.M. Jones, F.S. Fasoon, A. Mason and M.J. Heben, *Nanostruct. Mater.* **12** (1999) 83.
12. H. Cao, Z. Xu, D. Sheng, J. Hong, H. Sang and Y. Du, *J. Mater. Chem.* **11** (2001) 958.
13. M. Baumgartner and H. Kaesche, *Corros. Sci.* **29** (1989) 363.
14. C.J. Miller and M. Majda, *J. Electroanal. Chem.* **207** (1986) 49.
15. M. Schirmeisen and F. Beck, *J. Appl. Electrochem.* **19** (1989) 401.
16. U.R. Evans, 'The Corrosion and Oxidation of Metals' (Edward Arnold, London, 1960), p. 242.
17. K. Juttner, *Electrochim. Acta* **35** (1990) 1501.
18. D. Cambbell and J.R. White, "Polymer characterization – physical techniques' (Chapman & Hall, London, 1991), p. 132.
19. L.H.C. Mattoso and A.G. MacDiarmid, *in* J.C. Salomone (Ed.), 'Polymeric Materials Encyclopedia', Vol. 7 (CRC Press, New York, 1996), p. 5505.
20. D.C. Trivedi, *in* H.S. Nalva (Ed.), 'Conductive Polymers: Synthesis and Electrical Properties', Vol. 2 (John Wiley & Sons, New York, 1997), p. 537.
21. E.T. Kang, K.G. Neoh and K.L. Tan, *Prog. Polym. Sci.* **23** (1998) 277.